

## An apparatus for screening fire suppression efficiency of dispersed liquid agents<sup>☆</sup>

Jiann C. Yang\*, Michelle K. Donnelly, Nikki C. Privé,  
William L. Grosshandler

*Building and Fire Research Laboratory, National Institute of Standards and Technology, 100 Bureau Drive,  
Stop 8651, Gaithersburg, MD 20899-8651, USA*

Received 16 September 1999; received in revised form 10 July 2000; accepted 17 July 2000

---

### Abstract

The design, construction, demonstration, and operation of a bench-scale device capable of comparison screening the fire suppression efficiency of liquid agents are described in this paper. The apparatus is based on a well-characterized flame, a means to facilitate the introduction of liquid agents, and a way to generate liquid droplets. A porous cylinder in a counterflow diffusion configuration is used. A small-scale vertical wind tunnel, which allows for the delivery of a uniform flow of oxidizer to the burner and also assists in the delivery of liquid agent droplets to the flame, is used for the flow facility. Droplets are generated by a small glass nebulizer. The performance of the screening apparatus was evaluated using several liquid fire suppressants with different thermophysical properties. A test protocol is also proposed. Published by Elsevier Science Ltd.

*Keywords:* Water additives; Droplets; Diffusion flames; Fire suppression

---

### 1. Introduction

The recent ban on halon 1301 (CF<sub>3</sub>Br) production (as a result of its ozone depleting potential) has resulted in extensive search for its replacements and alternatives. The applications of fire suppression efficiency screening methods constitute an important aspect of this search process because good screening methods can facilitate the

---

<sup>☆</sup>Official contribution of the National Institute of Standards and Technology not subject to copyright in the United States.

\* Corresponding author. Tel.: +1-301-975-6662; fax: +1-301-975-4052.

*E-mail address:* jiann.yang@nist.gov (J.C. Yang).

identification, comparison, and selection of potential candidates for halon replacement. Most of the current methods for fire suppression efficiency screening (e.g., cup burners) are designed for evaluating fire suppressing agents that can be delivered in the form of vapor. Potential uses of liquid agents as replacements have been recently proposed in several applications (e.g., shipboard machinery spaces, engine compartments in armored vehicles). Therefore, there is a need for the development of a reliable screening method for liquid agents that can be delivered in droplet form. The objective of this work is to design, construct, and demonstrate a laboratory-scale apparatus that can perform the screening of liquid agents in a well-controlled experimental setting. The design of the apparatus is based on a well-characterized flame, a means to facilitate the introduction of small amounts of liquid agents, and a way to generate liquid droplets that can be entrained into the flame. The device can also be used to screen gaseous fire suppressants. In principle, the apparatus can be employed to screen powders by incorporating a powder delivery system in lieu of a liquid droplet generator.

In the literature, the experimental non-premixed configurations used for agent screening applications include: (1) counterflow cylindrical burners; (2) counterflow flat-flame burners; and (3) cup burners.

A porous cylindrical burner in a counterflow configuration has been extensively used to study flame structure [1–4] and flame extinction using inert gases [5], halons [6], and powders [6]. In such a configuration, the burner with fuel being injected uniformly from its surface is placed in a uniform oxidizer flow, and a diffusion flame is formed in the forward stagnation region of the burner. There are many advantages associated with the use of a counterflow cylindrical burner. The fuel and the oxidizer flows can be independently adjusted, if required. The flame is laminar, two-dimensional, and very stable in the forward stagnation region. The geometry of the burner and the flow field allow for relatively simple analysis of the forward stagnation region [7–13]. Both wake and enveloped flames can be easily maintained over a wide range of fuel and oxidizer flows. The flame is easily observed, and critical stages such as the blow-off limit (abrupt transition from an enveloped flame to a wake flame) can be ascertained with ease and high reproducibility. The flame front can be easily accessed by intrusive [2,3] or non-intrusive [8,13] probing techniques; thus, enabling detailed studies of flame structure, if desired. However, clogging of the porous burner surface due to soot deposition and/or condensed-phase suppressant may be a disadvantage if the burner is operated for a long period of time; cleaning or replacing the clogged burner may be required [6].

Another counterflow geometry, which involves the use of two opposed vertical ducts separating at a distance with fuel and oxidizer counterflowing toward each other to establish a flat flame, has recently been used for extinction studies with solid aerosols [14,15] and two-phase droplet spray flames [16, and references therein]. Although counterflow flat-flame burners possess all the operational merits of a counterflow cylindrical burner mentioned above, the operation of these burners is elaborate.

Cup burners, which are widely used for screening gaseous agents, have also been employed recently to study the suppression efficiencies of condensed-phase

Table 1  
Comparison of the operational characteristics of the three screening apparatus<sup>a</sup>

	Co-flow cup burner	Counterflow flat-flame burner	Counterflow cylindrical burner
Gaseous agent screening applications	x	x	x
Introduction of condensed-phase agent to flame for evaluation	xxx	xx	x
Characterization of condensed-phase agent in flame	xxx	xx	xx
Attainment of stable and repeatable flame	xx	x	x
Adjustment of strain rate and composition	xxx	x	x
Accessibility for flame diagnostics	x	x	x
Observation of flame extinction	x	x	x
Flame structure analysis	xxx	xx	xx
Amenability to modeling (with chemical reactions)	xxx	x	x
Attainment of adiabaticity	xxx	x	xx
Facility design	x	xxx	xx
Interpretation of results	x	xx	xx
Elimination of burner clogging	xx	x	xxx
Facility operation	x	xx	x
Simulation of flame behind bluff body	Impossible	Impossible	x

<sup>a</sup>Degree of difficulty: x – simple; xx – difficult; xxx – very difficult.

agents [17,18]; however, the presence of the cup makes the introduction and characterization of liquid agents difficult. In addition, the global strain rate of a pool flame established at the cup is not well defined.

Table 1 lists a comparison of the various operational characteristics among the three screening apparatus: the cup burner, the counterflow flat flame burner, and the counterflow cylindrical burner. Since the operation of a counterflow cylindrical burner is less complicated than that of a counterflow flat-flame burner and the experimental configuration facilitates the introduction of condensed-phase agents into the oxidizer stream, we make use of such a burner in our liquid agent screening apparatus.

## 2. Apparatus

There are three major elements in the apparatus: (1) a wind tunnel; (2) a porous cylindrical burner; and (3) a droplet generator. These three components will be briefly described in the following; detailed descriptions and the operation of the apparatus are provided in Ref. [19].

### 2.1. Wind tunnel

The wind tunnel is used to provide uniform oxidizer flow to the porous cylindrical burner at a low turbulence intensity and to facilitate the delivery of liquid agent droplets to the flame for testing. The wind tunnel is open-circuit (non-recirculating)

and is oriented vertically upwards. A schematic of the tunnel is shown in Fig. 1. The total length of the tunnel from the entrance of the diffuser to the exit of the test section is approximately 1.2 m. The tunnel, except the test section, is made of clear polycarbonate for visual observation of droplet transport toward the burner.

The test section has a cross-sectional area of 10 cm × 10 cm and a length of 20 cm. It is made of black-anodized aluminum with three borosilicate observation windows

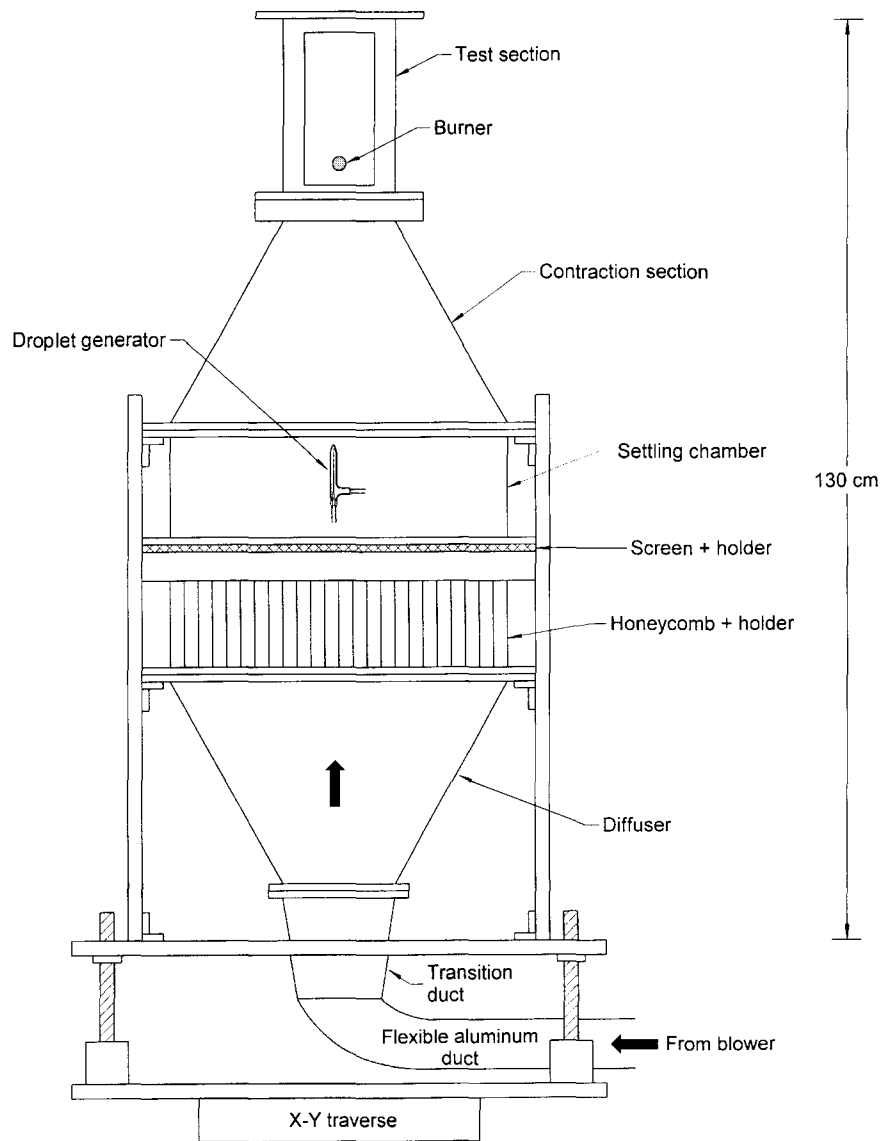


Fig. 1. A schematic representation of the wind tunnel.

mounted flush against the three walls of the test section. The combustion products from the burner are vented to an exhaust hood.

The wind tunnel is mounted on a  $x$ - $y$ - $z$  traverse mechanism which is used to position the burner with respect to the stationary optical set-up for droplet characterization at various locations near the burner.

The velocity profile in the test section obtained using a pitot tube was relatively flat ( $<0.5\%$  variation) except in the region near the walls (boundary layer thickness less than 1 cm). The combined standard uncertainty ( $u_c$ ) in the velocity measurement is 2 cm/s. Due to the limited frequency response of the pitot tube, the turbulence intensity level was not measured; however, the observation of a very stable laminar flame zone in the forward stagnation region of the burner provided a qualitative indication of low turbulence intensity. The volumetric flow rates are calculated using the measured average air velocities ( $V_0$ ) and the cross-sectional area of the test section.

## 2.2. Porous cylindrical burner

The design of the burner is based on several important criteria. The burner has to be robust, easily built, installed, and operated, and able to generate reliable screen test data.

The burner is a replaceable porous (20  $\mu\text{m}$  pores) sintered stainless steel standard  $\frac{1}{2}$ " UNF threaded cup filter with a length  $L$  of 3.18 cm, an inner diameter of 1.12 cm, and an outer diameter  $D$  of 1.58 cm. The advantage of this burner design over those used in the past is that burner replacement can be easily performed if partial or complete clogging of the porous burner surface occurs due to the deposition of soot particles or residue from liquid agents containing dissolved solids. The burner is screwed onto an extended water-cooled insert through which fuel is injected. The water is used to cool the burner to prevent damage to the porous surface structure and the fuel (propane) to prevent fuel pyrolysis prior to its ejection through the porous surface. A cut-away view of the burner interior is shown in Fig. 2.

The burner, together with the insert, does not span the entire test section of the wind tunnel. A cylindrical brass rod (same diameter as the burner) with internal water

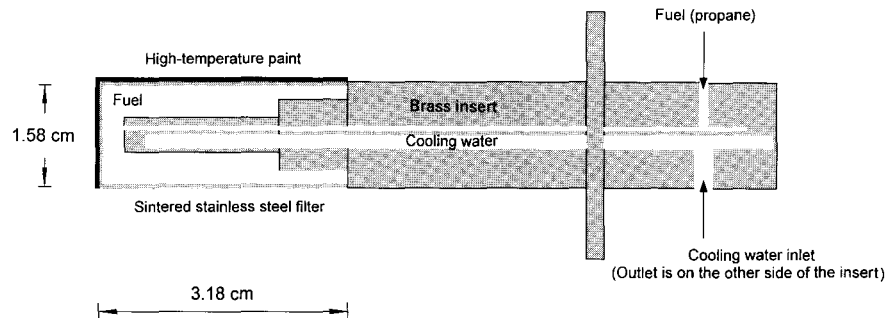


Fig. 2. A cut-away view of the burner insert.

cooling is inserted from the opposite wall and is used as an extension so that the burner assembly can be treated as a single cylinder across the test section.

The side and downstream 180° portions of the burner surface are coated with a thin layer of high-temperature resistant black paint to prevent fuel ejection into the wake region. The high-pressure drop across the porous sintered surface assures a very uniform fuel flow over the burner surface.

### 2.3. Droplet generator

A small glass nebulizer is employed in the screening apparatus to generate a fine mist of droplets. This type of nebulizer has found applications in inductively-coupled plasma (ICP) atomic emission spectroscopy and is commercially available. A schematic of the nebulizer is shown in Fig. 3. Aerodynamic break-up of a liquid stream issued from the capillary by high-velocity air causes the formation of a fine mist of droplets. Because of the large opening ( $\approx 100\ \mu\text{m}$ ) of the capillary, the nebulizer can be used with a wide range of liquids, including those with a relatively high salt concentration. The large capillary opening makes the nebulizer less prone to clogging. Fluid is fed to the nebulizer by a small, programmable syringe pump. Air is supplied to the shell of the nebulizer by a mass-flow controller. The resulting mist is entrained upwards toward the flame by the air flowing in the tunnel. The atomizing air flow is set at 0.25 l/min, which is the highest flow that can be used without disturbing the flame at the burner. Because of this limit, the atomization efficiency (for all the fluids reported herein) of the nebulizer *may* deteriorate when the liquid delivery

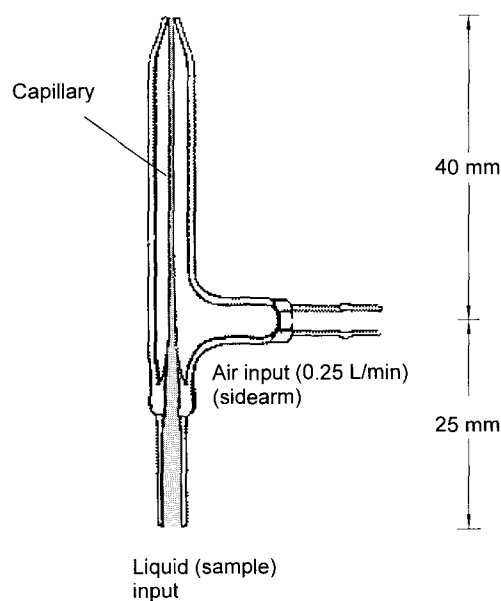


Fig. 3. A schematic representation of the nebulizer.

rate is increased beyond  $1.3 \text{ cm}^3/\text{min}$ ; that is, larger droplets are generated that may not be easily entrained upward by the air flow in the tunnel.

The nebulizer is mounted in the settling chamber of the wind tunnel and is approximately 42 cm upstream of the burner. The presence of the nebulizer in the wind tunnel does not create any significant perturbation or blockage effect on the oxidizer flow field near the burner because the velocity profile at the test section and the flame characteristics do not change with or without the presence of the nebulizer in the flow stream. In addition, deposition of droplets on the wall of the contraction section was not visually observed.

### 3. Results and discussion

#### 3.1. Burner characterization

For a given burner diameter, there are only two important parameters, fuel ejection velocity ( $V_f$ ) and air velocity ( $V_o$ ) in the wind tunnel, that govern the performance of the burner [1,2].

Under certain flow conditions, a thin, laminar, two-dimensional blue flame is established at a distance in front of the cylinder surface. An example is given in Fig. 4(a). As the fuel ejection velocity is decreased or the air velocity is increased, the flame slowly approaches the cylinder surface, and eventually the flame is abruptly blown off from the stagnation region, and a wake flame, an example of which is shown in Fig. 4(b), is established. Conversely, with increasing fuel velocity or decreasing air velocity, the flame zone gradually moves away from the cylinder surface, and eventually a laminar two-dimensional flame can no longer be sustained.

When the air velocity is very small and the fuel velocity is large, the flame zone becomes thicker, and an inner luminous yellow zone and an outer blue zone appear. When the air velocity is very large and reaches a critical value, the flame can never be stabilized, irrespective of the fuel ejection velocity.

Fig. 5 shows the various flame stability regions of the burner obtained from the test facility. Each data point on the upper curve was obtained by maintaining a fixed fuel flow and increasing the air flow until blow-off occurred. The fuel ejection velocity is calculated by dividing the fuel volumetric flow by the available fuel ejection area of the burner surface, which is equal to  $\pi DL/2$ . The regions below and above the curve correspond to the existence of a stable enveloped blue flame and a wake flame, respectively. There is a critical air velocity above which a stable enveloped flame can no longer be established, irrespective of the fuel flow. This critical blow-off velocity depends on fuel type and burner diameter [1]. Each data point on the lower curve was obtained by increasing the fuel ejection rate at a fixed oxidizer flow until a luminous yellow zone appeared. The conditions below this curve represent the existence of a yellow luminous zone.

For our proposed *liquid* screening applications, the fuel flow is always fixed at 21/min, which corresponds to an ejection velocity of 4.2 cm/s. The selection of 21/min is partly to eliminate the effect of fuel flow on blow-off velocity. In addition, higher fuel

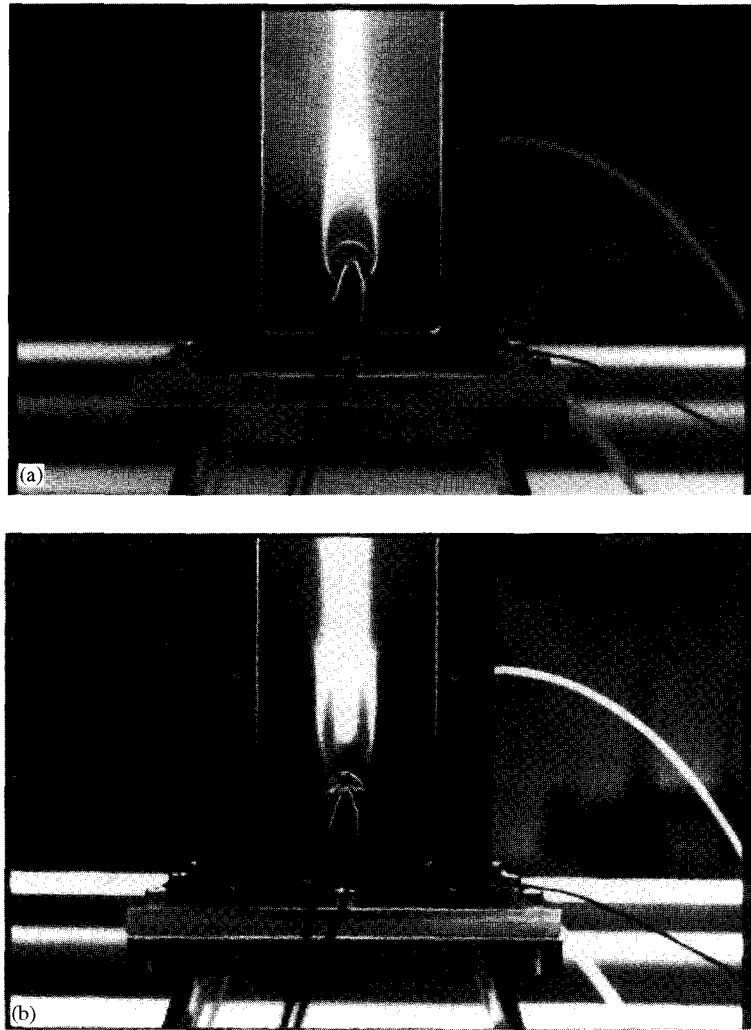


Fig. 4. Photographs of an enveloped flame (a) and a wake flame (b).

injection velocity reduces heat loss to the burner [1]. However, a higher fuel injection velocity requires higher air velocity to achieve a stable blue flame (see Fig. 5). The advantage of having a higher operating air flow is that it facilitates the droplet transport to the flame. It also enables the use of larger droplets without having them settled out by gravity. The disadvantage is that a higher air flow results in a higher global strain rate of the flame, which may not be representative of a fire.

To assess the burner performance due to burner-to-burner variation, blow-off experiments were performed using four different burners. Based on two independent repeated observations, the overall coefficient of variation in the measurements of the air velocities at blow-off is 2%.

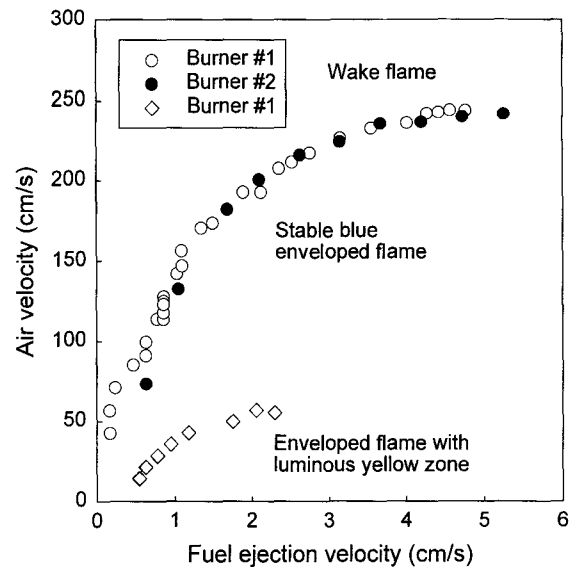


Fig. 5. Flame stability curve.

### 3.2. The characterization of the droplet generator

Since the droplets are propelled upwards, there are several limitations to the droplet sizes that can be used in the experiments. The first limitation is that for a given burner size, there is a maximum (critical) air flow (as discussed previously) above which the experiments cannot be performed because an enveloped flame cannot be initially established. However, this limitation can be easily alleviated by using a larger burner which results in a higher critical blow-off velocity [1]. The second limitation is that the droplet generator is located in the settling chamber where the air velocity is low because of the large cross-sectional area of the chamber. If the initial droplet velocity is small, it is likely that the droplet (depending on its initial size) will not be entrained upwards by the low-speed air, and the droplet will eventually fall down due to gravity before reaching the test section. The desirable droplet size for the experiments can be estimated by using the equation of motion for a droplet [20]. The calculated results demonstrate that a 60  $\mu\text{m}$  droplet can easily be entrained upwards by the existing air flow in the settling chamber.

An Aerometrics<sup>1</sup> two-component phase Doppler particle analyzer (PDPA) with a Doppler signal analyzer (DSA) was used to measure droplet size and velocity distributions. The measurements were made at several positions near the droplet generation device and near the burner to assess the uniformity of the small dispersed droplet spray.

<sup>1</sup> Certain commercial products are identified in this paper in order to specify adequately the equipment used. Such identification does not imply recommendation by the National Institute of Standards and Technology, nor does it imply that this equipment is the best available for the purpose.

PDPA measurements of the nebulizer spray were taken on the centerline, 2 cm downstream of the nebulizer exit. Air was supplied to the nebulizer at 0.25 l/min, and de-ionized water was used as the calibration liquid. The liquid flow was varied from 0.3 to 1.2 cm<sup>3</sup>/min. Fig. 6 is an example of one set of results taken at a liquid flow of 0.5 cm<sup>3</sup>/min. The nebulizer creates droplets with a range of diameters, as evident in the diameter histogram in the figure. In the measurements, the nebulizer was pointed upward in the opposite direction of the vertical velocity prescribed by the orientation of the PDPA transmitter. In Fig. 6, Channels 1 and 2 represent the vertical and horizontal droplet velocity components, respectively.

PDPA measurements were also taken on the centerline at the burner location. Since the experiment protocol requires the blower air speed to increase until blow-off occurs, it is necessary to determine if such an increase could result in secondary disintegration of the droplets due to increasing aerodynamic forces on the droplets. Droplet size measurements were taken at blower air speeds of 111 and 179 cm/s. The change in blower air speed within the range for the experiments was found to have a negligible effect on the diameter of the droplets which reached the burner. The Sauter mean diameter, defined as the ratio of spray droplet volume to droplet surface area, is in the range of 25–35 μm for all air velocities and water application rates. There is a slight tendency for the droplet diameter to increase with liquid delivery rate. The standard uncertainty (based on repeated measurements) is 2 μm.

Droplet size measurements were also performed by moving the nebulizer to different off-center locations in the settling chamber to account for possible misalignments, and this was found to have no effect on the droplet size near the burner.

The droplet number densities were also measured at four locations (1 cm upstream of the burner): (1) centerline, (2) 0.5 cm off centerline, (3) 1.0 cm off centerline, and (4) 1.5 cm off centerline. There was a ≈ 40% variation in the measurements, with the highest number density on the centerline and the lowest at 1.5 cm off centerline.

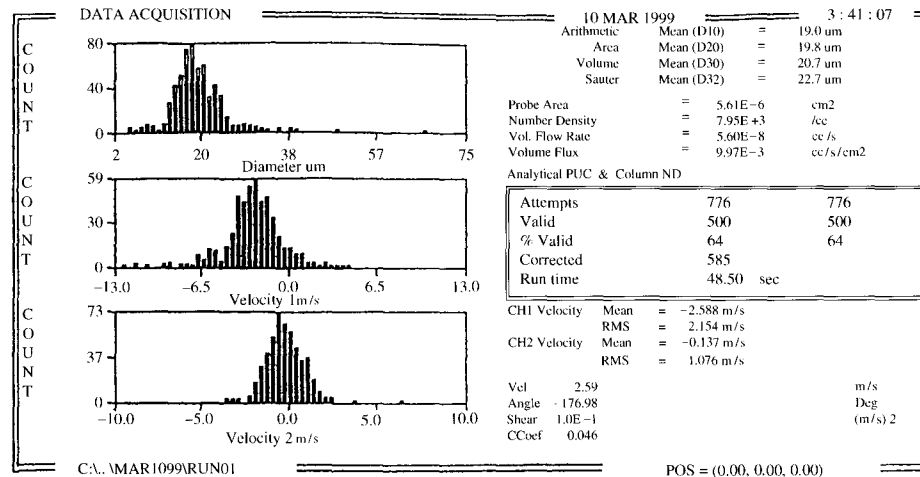


Fig. 6. Sample measurement of the mist from the nebulizer using the two-component PDPA at the centerline location, 2 cm downstream of the nebulizer exit.

Since the atomizing characteristics of the nebulizer depend on the physical properties of the fluids [21], different droplet size distributions may result when different test fluids are used; this could complicate the interpretation of the screening results by introducing the additional effect of droplet diameter. A series of measurements was performed using the PDPA to determine the dependence of droplet size on the physical properties of the test fluids. Several surrogate fluids (water, 30% and 45% (mass fraction) potassium lactate, and 1 and 2 g/l sodium dodecyl sulfate (SDS)) were used to simulate variations in densities, viscosities, and surface tensions. Table 2 lists some of their physical properties. Fig. 7 shows the PDPA measurement results on the centerline, 2 cm downstream of the nebulizer exit for liquid flows

Table 2  
Physical properties of surrogate fluids at 20°C

Fluid	Density (g/cm <sup>3</sup> ) ± 0.01	Viscosity <sup>a</sup> (g/s cm) ± 0.001	Surface tension <sup>b</sup> (dyne/cm) ± 1
Distilled water	1.00	0.010	72
30% potassium lactate	1.15	0.025	66
45% potassium lactate	1.23	0.038	68
1 g/l SDS	0.98	0.0095	52
2 g/l SDS	0.96	0.0093	38

<sup>a</sup>Measured using a Cannon® Glass Capillary Viscometer.

<sup>b</sup>Measured using a DuNouy® Tensiometer (Model No. 70535, CSC-Scientific Co., Inc.).

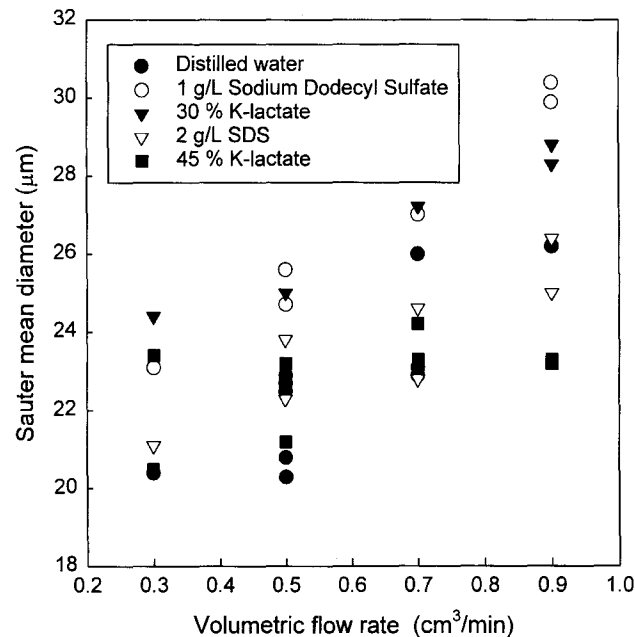


Fig. 7. Droplet diameter measurements of various fluids using the PDPA at the centerline location, 2 cm downstream of the nebulizer exit.

between 0.3 and 0.9 cm<sup>3</sup>/min. In all cases, the Sauter mean diameters only vary between 20 and 30 μm.

### 3.3. Screening of liquid agents

The transition from a stable enveloped blue flame to a wake flame, that is the air velocity at blow-off, is used as a criterion for screening the fire suppression effectiveness of various fire suppressants; the higher the air blow-off velocity, the less effective the fire suppressant.

There are two ways to perform the screen experiments: (1) increasing the air flow at a fixed liquid agent application rate until blow-off occurs, and (2) increasing the liquid agent application rate at a fixed air flow until blow-off occurs. The former was selected because the procedure requires less agent and there is no need to correct for the lag time from changing the syringe pump setting (to increase the liquid flow) to attaining a steady liquid delivery rate.

The screening procedure is as follows. A blow-off experiment without agent is first conducted to check the burner performance, followed by a blow-off experiment with a fixed agent application rate. This process is shown schematically as the vertical line in Fig. 8. The blow-off velocities are used to provide a *relative* ranking of various liquid agents.

Several test fluids (water, skim milk, 30% sodium iodide, and 30 and 60% potassium lactate) have been used to evaluate the performance of the screening apparatus. Milk is known to be a fire suppressant [22], sodium iodide was selected because it

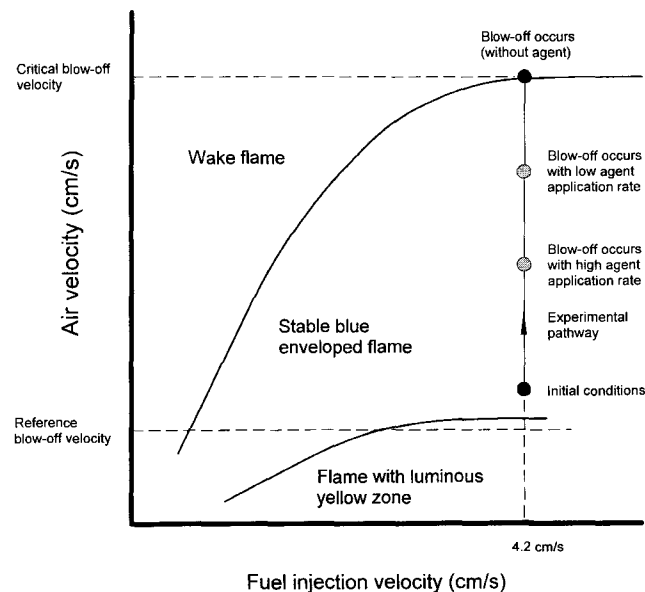


Fig. 8. A schematic representation illustrating the experimental procedure.

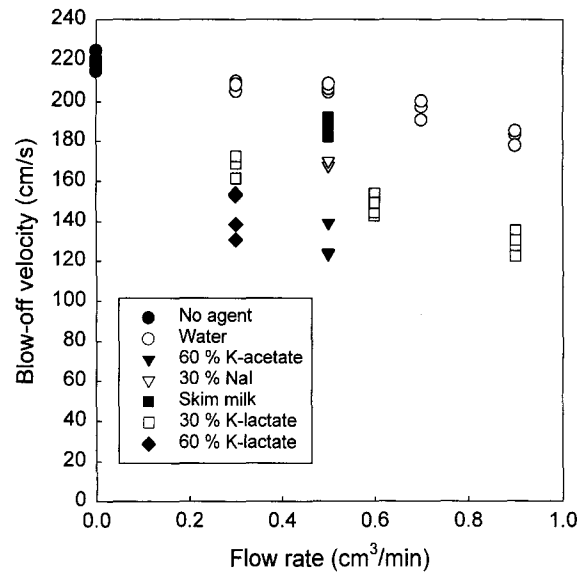


Fig. 9. Screening results using different types of fluids.

may be more effective than sodium bromide [23], and potassium lactate has been demonstrated to be more effective than water [23]. Fig. 9 shows the screening results using these test fluids. Each data point represents one test. For a given fluid, increasing the liquid application rate decreases the blow-off velocity. As expected, a mass fraction of 60% potassium lactate is more effective than 30% potassium lactate. Water is the least effective when compared to skim milk, 30% sodium iodide, and 60% potassium acetate. In this set of data, the coefficient of variation from run-to-run using the liquid screening apparatus was estimated to be better than 20%.

There are many liquid delivery rates that one can use in the screening procedure described above, and a reference delivery rate is needed to assess the fire suppression effectiveness of various liquid agents in a consistent way and under conditions commensurate with a fire. Since cup burners have been used for estimating gaseous agent concentrations required to extinguish a fire, we have developed the following protocol, which is based on the conditions commensurate with the cup-burner results for nitrogen.

The average propane cup-burner value for nitrogen is 32% (mass fraction) [17]. This value corresponds to a blow-off velocity of  $\approx 30$  cm/s from the experimental results obtained using the same porous cylindrical burner with nitrogen added to the air stream [19]. At this velocity and a propane flow of 21/min, a flame cannot be stabilized in the desired blue enveloped flame region (refer to Fig. 5). In addition, the experimental protocol calls for increasing the air velocity (i.e., moving away from 30 cm/s) until blow-off at a fixed fluid delivery rate. To compare the results obtained from the cylindrical burner to conditions commensurate with cup-burner results, extrapolation to lower air velocity (strain rate) is required.

Note that nitrogen is selected as a reference gas simply due to the availability of suppression data for the cylindrical burner [19]. Similar reference blow-off velocities will be obtained when the cup-burner results for other gases are used because at the *same* low global strain rate in a counterflow flat-flame burner, the agent extinction concentrations agree well with the measurements obtained from a cup burner [17].

Fig. 10 demonstrates the proposed extrapolation mechanism for obtaining the reference liquid application rate. Note that the linear extrapolation process is an approximation because the relationship between blow-off velocity and agent application rate may not be linear at low blow-off velocities. A blow-off air velocity without fluid application is obtained, followed by a blow-off experiment with a given fluid application rate (or a series of blow-off experiments with different application rates). The fluid delivery rate at an air velocity of 30 cm/s is then deduced by linear extrapolation. Based on our experience, an application rate between 0.6 and 1 cm<sup>3</sup>/min appears to be appropriate, which is a compromise between minimizing the fluid consumption for a test and attaining a blow-off velocity close to the reference blow-off velocity of 30 cm/s.

Once the application rate corresponding to the reference blow-off velocity is deduced, the reference mass flow rate of the liquid agent,  $\dot{m}_{\text{agent, ref}}$ , can be calculated using the liquid density. The reference mass fraction of the liquid agent in the air stream is then

$$Y_{\text{agent, ref}} = \frac{\dot{m}_{\text{agent, ref}}}{\dot{m}_{\text{agent, ref}} + \dot{m}_{\text{air, ref}}}, \quad (1)$$

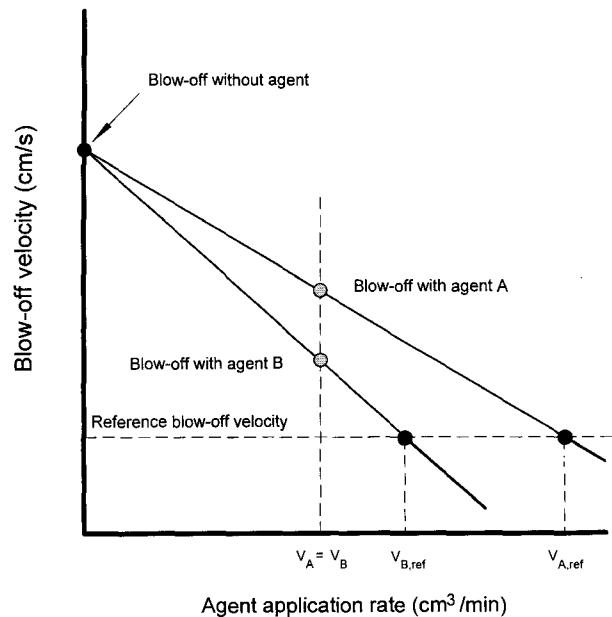


Fig. 10. A schematic representation illustrating the extrapolation for obtaining agent application rates at the reference blow-off velocity.

where  $\dot{m}_{\text{air, ref}}$  is the mass flow of air, calculated based on the cross-sectional area of the test section and 30 cm/s.

Note that in writing Eq. (1), it is implicitly assumed that the droplets are homogeneously dispersed in the carrier phase (air). If the droplets are not homogeneously dispersed across the total cross-sectional area, the calculated agent mass fraction will be underestimated because  $\dot{m}_{\text{air, ref}}$  is overestimated. The effective area can be considered as the effective coverage area of the mist in the test section. Depending on the effective coverage area, a difference of a factor of *two* to *three* in the calculated liquid mass fraction can result. By placing a filter paper over the exit of the test section for a short duration with the wind tunnel operating (without the burner) and the nebulizer with a dye added to the fluid, the droplet-impact (color) pattern on the filter paper can be visualized and used as an indicator to determine the mist coverage area in the test section. The color pattern, which is approximately circular, indicates that the mist from the nebulizer completely covers the burner and its vicinity. The mist coverage area was estimated to be ca. 40% of the total cross-sectional area of the test section for all the fluids used in our screening tests. In addition, the droplet-impact (color) pattern was concentrated in the center and gradually diffused outward. This observation was in qualitative agreement with the droplet number density measurements using the PDPA.

Table 3 summarizes the calculations of the reference agent mass fraction in air using the screening results from Fig. 9, and the proposed approach described above without mist coverage area correction. Average values of the blow-off velocities were used in the extrapolation. For cases where blow-off velocities at more than one liquid application rates are available, linear regressions were used to extrapolate the reference blow-off velocities. When data with one application rate were available, simple linear extrapolation was applied to obtain the reference blow-off velocities.

The last column of Table 3 lists the ranking indices relative to water. For example, the 60% K-acetate and K-lactate solutions are considered to be four times more effective than water at the reference blow-off velocity. The ranking (60% K-lactate vs. water) is consistent with the suppression results reported in Ref. [23] using a small JP-8 pool fire and a commercial spray gun.

Table 3  
Calculated nominal agent mass fractions at reference blow-off air velocity of 30 cm/s

Agent	$V_{\text{agent, ref}}$ (cm <sup>3</sup> /min)	Agent density (g/cm <sup>3</sup> ) at 20°C	$\dot{m}_{\text{agent, ref}}$ (g/s)	Nominal agent mass percent (%)	$\frac{\dot{m}_{\text{water, ref}}}{\dot{m}_{\text{agent, ref}}}$
Water	4.62	1.00	0.08	2.6	1.0
60% K-acetate	0.99	1.34	0.02	0.8	4.0
30% NaI	1.76	1.29	0.04	1.3	2.0
Skim milk	2.78	1.01	0.05	1.6	1.6
30% K-lactate	1.74	1.15	0.04	1.2	2.0
60% K-lactate	0.71	1.33	0.02	0.6	4.0

Irrespective of the uncertainty associated with the estimated nominal agent mass concentration, water and the aqueous agents studied here are found to be more effective than  $\text{CF}_3\text{Br}$ , compared to the propane cup-burner value (mass fraction of 17% [17]) for  $\text{CF}_3\text{Br}$ . The computational study by Lentati and Chelliah [24] also demonstrates that  $20\ \mu\text{m}$  water droplets are more effective in extinguishing an opposed-flow methane diffusion flame than  $\text{CF}_3\text{Br}$ , which is in qualitative agreement with the results reported here.

Care should be exercised when interpreting the agent concentrations from the screening results in Table 3, which were obtained using an idealized laboratory flame and a droplet delivery system such that the transport of fine liquid droplets to the flames is not a factor in determining the suppression effectiveness. In the case of real fires, droplet entrainment and transport to the fire can significantly affect the liquid agent mass concentration required to suppress a fire, especially in highly obstructed enclosure fires.

#### 4. Conclusions

An apparatus for screening liquid agents delivered in droplet form has been developed. The performance of the apparatus has been characterized using fluids with different thermophysical properties and fire suppression effectiveness. The apparatus is robust and easy to operate. The droplet delivery system is designed to handle small quantity of liquid sample; this requirement is critical because potential new liquid agents may be synthesized and available in minute quantity for testing. For all the test results reported here,  $10\ \text{cm}^3$  of sample is needed to perform a *rapid* screen (with at least one repeat). The apparatus can also be used to screen gaseous agents. When a powder delivery system is integrated into the current apparatus, the facility, in principle, can be employed to screen powder agents.

#### Acknowledgements

The work is supported by the Department of Defense's Next Generation Fire Suppression Technology Program (NGP), funded by the DoD Strategic Environmental Research and Development Program (SERDP). Dr. Richard G. Gann is the Technical Program Manager. The authors would also like to thank Drs. Marc Rumminger and John Widmann for reading the manuscript and providing many useful comments and the referees who performed a careful review and helped to improve the contents of the paper.

#### References

- [1] Tsuji H, Yamaoka I. The counterflow diffusion flame in the forward stagnation region of a porous cylinder. Eleventh International Symposium on Combustion, The Combustion Institute, Pittsburgh, PA, 1967. p. 979–84.

- [2] Tsuji H, Yamaoka I. The structure of counterflow diffusion flames in the forward stagnation region of a porous cylinder. Twelfth International Symposium on Combustion, The Combustion Institute, Pittsburgh, PA, 1969. p. 997–1005.
- [3] Tsuji H, Yamaoka I. Structure analysis of counterflow diffusion flames in the forward stagnation region of a porous cylinder. Thirteenth International Symposium on Combustion, The Combustion Institute, Pittsburgh, PA, 1971. p. 723–31.
- [4] Tsuji H. Counterflow diffusion flames. *Prog Energy Comb Sci* 1982;8:93–119.
- [5] Ishizuka S, Tsuji H. An experimental study of effect of inert gases on extinction of laminar diffusion flames. Eighteenth International Symposium on Combustion, The Combustion Institute, Pittsburgh, PA, 1981. p. 695–703.
- [6] Milne TA, Green CL, Benson DK. The use of the counterflow diffusion flame in studies of inhibition effectiveness of gaseous and powdered agents. *Comb Flame* 1970;15:255–64.
- [7] Dixon-Lewis G, David T, Gaskell PH, Fukutani S, Jinno H, Miller JA, Kee RJ, Smooke MD, Peters N, Effelsberg E, Warnatz J, Behrendt F. Calculation of the structure and extinction limit of a methane–air counterflow diffusion flame in the forward stagnation region of a porous cylinder. Twentieth International Symposium on Combustion, The Combustion Institute, Pittsburgh, PA, 1984. p. 1893–904.
- [8] Dreier T, Lange B, Wolfrum J, Zahn M, Behrendt F, Warnatz J. CARS measurements and computations of the structure of laminar stagnation-point methane–air counterflow diffusion flames. Twenty-first International Symposium on Combustion, The Combustion Institute, Pittsburgh, PA, 1986. p. 1729–36.
- [9] Peters N, Kee RJ. The computation of stretched laminar methane–air diffusion flames using a reduced four-step mechanism. *Comb Flame* 1987;68:17–29.
- [10] Olson SL, T'ien JS. A theoretical analysis of the extinction limits of a methane–air opposed-jet diffusion flame. *Comb Flame* 1987;70:161–70.
- [11] Dixon-Lewis G, Missaghi M. Structure and extinction limits of counterflow diffusion flames of hydrogen–nitrogen mixtures in air. Twenty-second International Symposium on Combustion, The Combustion Institute, Pittsburgh, PA, 1988. p. 1461–70.
- [12] Chen CH, Weng FB. Flame stabilization and blowoff over a porous cylinder. *Combust Sci Technol* 1990;73:427–46.
- [13] Sick V, Arnold A, Dießel E, Dreier T, Ketterle W, Lange B, Wolfrum J, Thiele KU, Behrendt F, Warnatz J. Two-dimensional laser diagnostics and modeling of counterflow diffusion flames, Twenty-third International Symposium on Combustion, The Combustion Institute, Pittsburgh, PA, 1990. p. 495–501.
- [14] Fleming JW, Reed MD, Zegers EJP, Williams BA, Sheinson RS. Extinction studies of propane/air counterflow diffusion flames: the effectiveness of aerosols. Halon Options Technical Working Conference, Albuquerque, New Mexico, USA, May 12–14, 1998. p. 403–14.
- [15] Chelliah HK, Krauss RH, Zhou H, Lentati AM. Characterization of physical, thermal, and chemical contributions of sodium bicarbonate particles in extinguishing counterflow nonpremixed flames. Proceedings of the 5th ASME/JSME Joint Thermal Engineering Conference, San Diego, California, USA, March 1999.
- [16] Li SC. Spray Stagnation Flames. *Prog Energy Comb Sci* 1997;23:303–47.
- [17] Grosshandler WL, Gann RG, Pitts WM. Evaluation of alternative in-flight fire suppressants for full-scale testing in simulated aircraft engine nacelles and dry bays. NIST SP861, U.S. Department of Commerce, Washington DC, April 1994.
- [18] Shilling H, Dlugogorski BZ, Kennedy EM. Extinction of diffusion flames by ultrafine water mist doped with metal chlorides. Proceedings of the Sixth Australasian Heat and Mass Transfer Conference, Sydney, Australia, December 9–12, 1996. p. 275–82.
- [19] Yang JC, Donnelly MK, Privé NC, Grosshandler WL. Dispersed liquid agent fire suppression screen apparatus. NISTIR 6319, U.S. Department of Commerce, Washington DC, July 1999.
- [20] Yang JC, Donnelly MK, Privé NC, Grosshandler WL. Fire suppression efficiency screening using a counterflow cylindrical burner. Proceedings of the 5th ASME/JSME Joint Thermal Engineering Conference, San Diego, California, USA, March 1999.

- [21] Bayvel L, Orzechowski Z. Liquid atomization. Washington DC: Taylor & Francis, 1993.
- [22] Rossotti H. Fire. Oxford: Oxford University Press, 1993.
- [23] Finnerty AE, McGrill RL, Slack WA. Water-based halon replacement sprays. ARL-TR-1138, U.S. Army Research Laboratory, Aberdeen Proving Ground, Maryland, July 1996.
- [24] Lentati AM, Chelliah HK. Physical, thermal, and chemical effects of fine-water droplets in extinguishing counterflow diffusion flames. Twenty-Seventh International Symposium on Combustion, The Combustion Institute, Pittsburgh, PA, 1998. p. 2839–46.